CHAPTER IX

VERTICAL STABILITY

In the previous chapter we have considered the atmosphere in hydrostatic equilibrium. It is obvious that this type of equilibrium does not imply a thermodynamic equilibrium; for instance, the vertical gradient of temperature will imply vertical heat conduction. In the real atmosphere heat will also be lost or gained by radiative processes. If vertical equilibrium is not prevalent, we should consider a third type of heat transport process: turbulent conduction. Conduction by molecular diffusion is a very slow process, negligible for all practical purposes, so that it need not concern us. Conduction by radiation is more important by several orders of magnitude, and it is a legitimate question to consider if radiative processes play a major role in determining the vertical distribution of temperature. Calculations for an atmospheric column which would receive radiative energy through the base, while losing the same amount from the top (admittedly a gross over-simplification of actual radiative processes), lead to a steady distribution such as indicated by the dashed curve of Figure IX-1. On the other hand, if we assume, in addition, a thorough vertical mixing, up to a level indicated by a discontinuity (tropopause), a distribution such as that of the full curve would be obtained. The real atmospheric stratifications are reasonably similar to this curve, especially for average conditions in temperate and tropical latitudes. The vertical turbulent transport of heat is thus a major factor

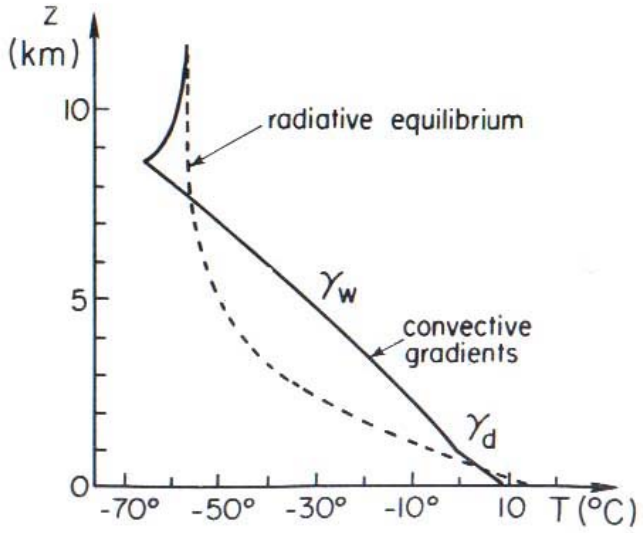

Fig. IX-1. Curve of radiative equilibrium and curve of convective lapse rates resulting from eddy diffusion (according to Emden).

determining the temperature distribution. In fact, when this mechanism is active, it may again be one or more orders of magnitude more efficient than the radiative transfer in determining local rates of change of temperature.

Apart from these considerations on energy transport, the vertical motions in the atmosphere are associated with weather disturbances and are therefore of primary importance to the meteorologist. Horizontal air motions can also not be neglected, and are particularly important on the time scale of day-to-day temperature changes.

In this chapter we shall investigate the conditions of vertical stability and instability in the atmosphere, first by assuming virtual infinitesimal displacements from equilibrium at one point, then by looking into the consequences that finite vertical displacements of isolated air masses may have, and finally by considering vertical movements of extensive layers. We shall also consider the internal and potential energies of air columns, as well as the consequences of radiative processes.

In order to avoid confusion whenever this is liable to occur, we shall use different symbols for geometric and for process derivatives and differentials. In the first case we shall substitute the symbol δ for d (e.g.: writing δz, $\delta T/\delta\phi$, etc.), while we shall leave the usual d for the latter variations (e.g.: $\mathrm{d}z$, $\mathrm{d}T/\mathrm{d}\phi$, etc.).

9.1. The Parcel Method

We shall now investigate the stability conditions regarding virtual vertical displacements of an atmospheric parcel in an environment which will be assumed to be in hydrostatic equilibrium.

The parcel is initially a part of the atmosphere, not different from any other at the same level. But it becomes an individualized portion as soon as it is assumed to start a displacement, while the environment remains at rest.

We shall denote by *reference level* the initial level of the parcel. The variables of the parcel will be distinguished by a prime (e.g., T') from those of the environment (T).

A number of simplifying assumptions are adopted in this method. It is supposed that:

(1) the parcel maintains its individuality during its movement, without mixing with the surrounding air,

(2) the movement of the parcel does not disturb the environment,

(3) the process is adiabatic, and

(4) at every instant the pressures of the parcel and of the environment for a given level are equal.

The first hypothesis, while reasonable when we consider infinitesimal virtual displacements, becomes quite unrealistic for finite displacements, and for this reason the data obtained in these cases are only semi-quantitative and must be corrected by empirical factors. The second assumption obviously cannot hold rigorously, since the ascent of an air mass must be compensated by the descent of other parts of the atmosphere; the approximation is good for isolated convection (when the disturbance of the environment is negligible) (cf. Section 8). The third hypothesis is reasonable, because

the heat conduction processes in the atmosphere (turbulent diffusion, radiation, molecular conduction) are in general slow compared to convective movements. Pressure quickly attains equilibrium, and therefore the last hypothesis is also good, provided the motions are not so violent that hydrodynamic perturbations become appreciable.

Taking into account these considerations, it is clear that, although the method leads to correct criteria for vertical equilibrium when only infinitesimal virtual displacements are considered (with the restriction mentioned with respect to the second assumption), it will lead to quantitative values in considerable error when finite displacements are considered. Even in these cases, however, it sheds considerable light on significant aspects of vertical instability and gives correct qualitative conclusions.

9.2. Stability Criteria

Let us consider a parcel displaced from its initial position (reference level), and it environment at its new level. As the environment is in equilibrium, Chapter VIII, Equation (19) must hold:

$$\frac{\delta p}{\delta z} + g\varrho = 0 . \tag{1}$$

The parcel, on the other hand, in general will not be in equilibrium: it will be subject to a force per unit mass equal to the resultant of the forces of gravity and of the pressure gradient. The first one is $-g$, where the sign indicates that it points downwards. To calculate the second one, we consider an infinitesimal layer of thickness δz from a column of unit cross section (see Figure IX-2). The force $-(\delta p/\delta z)\delta z = -(\delta p/\delta z)V'$ acts upon it, where V' is the volume of the layer. Dividing by V', we have the force per unit volume $-\delta p/\delta z$ (where p is the same as in Equation (1), according to the fourth assumption). The resultant of both forces will produce an acceleration $\ddot{z}$ (the dots meaning differentiation with respect to time), so that, per unit volume, we shall have the equation

$$\frac{\delta p}{\delta z} + g\varrho' = -\varrho'\ddot{z} . \tag{2}$$

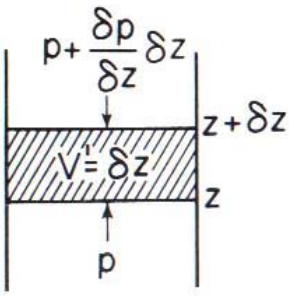

Fig. IX-2. A parcel, considered as a layer of an atmospheric column.

Subtracting Equation (2) from (1):

$$\ddot{z} = g\frac{\varrho - \varrho'}{\varrho'} \tag{3}$$

which, taking into account the gas law, and the definition of virtual temperature, can also be written

$$\ddot{z} = g\frac{v' - v}{v} = g\frac{T'_v - T_v}{T_v}. \tag{4}$$

This expression gives thus the force per unit mass acting on the parcel, due to both gravity and the pressure gradient. It is frequently called the *buoyancy* on the parcel, and written with the symbol B. In what follows we shall use the expression with virtual temperatures. We also have

$$T_v = T_{v_0} - \gamma_v\,\delta\phi\,; \qquad T'_v = T'_{v_0} - \gamma'_v\,\mathrm{d}\phi' \tag{5}$$

where the subscript 0 refers to the reference level. Obviously, $T'_{v_0} = T_{v_0}$ and $\delta\phi = \mathrm{d}\phi' = g\,\mathrm{d}z$. Therefore:

$$T_v = T_{v_0} - \gamma_v g\,\mathrm{d}z\,; \qquad T'_v = T_{v_0} - \gamma'_v g\,\mathrm{d}z \tag{6}$$

and

$$T'_v - T_v = (\gamma_v - \gamma'_v) g\,\mathrm{d}z\,. \tag{7}$$

Substituting into Equation (4):

$$\ddot{z} = \frac{g^2}{T_v}(\gamma_v - \gamma'_v)\,\mathrm{d}z\,. \tag{8}$$

This formula shows that, if $\gamma'_v < \gamma_v$, the parcel will acquire an acceleration $\ddot{z}$ after the virtual displacement of the same sign as the displacement $\mathrm{d}z$; it will tend to move away from the reference level, with increasing acceleration: this is the case of instability (positive buoyancy). If $\gamma'_v > \gamma_v$, $\ddot{z}$ and z will have opposite signs and the parcel will tend to return to its original position (negative buoyancy): this is the case of stability. If $\gamma'_v = \gamma_v$, the equilibrium is indifferent, and after being displaced, the parcel will remain in its new position. These stability conditions are summarized in the relation:

$$\gamma_v \gtrless \gamma'_v \tag{9}$$

where
- $>$ corresponds to instability
- $=$ corresponds to indifference (neutral or zero stability)
- $<$ corresponds to stability.

The aerological sounding gives the variables T, p, U_w for each height; with these data γ_v can be calculated, and at the same time virtual displacements can be imagined and the resulting process lapse rate can be calculated. The comparison is extremely simple with a diagram, and permits the use of the criterion (9), as we shall see in Section 5.

9.3. Lapse Rates for Atmospheric Ascents

Before proceeding further with the stability criteria, we shall consider now the expressions for the thermal gradient for a dry adiabatic ascent γ_d, moist (air) adiabatic ascent γ_m, polytropic ascent γ_p and saturated adiabatic ascent γ_w. As the ascent of the parcel is adiabatic, the parcel will undergo one of these processes, according to the humidity conditions.

For an adiabatic process without condensation or evaporation:

$$\delta q = 0 = \mathrm{d}h - v\,\mathrm{d}p = c_p\,\mathrm{d}T - v\,\mathrm{d}p \tag{10}$$

and assuming hydrostatic equilibrium (i.e., assuming that the vertical motion is slow enough to consider the process as quasistatic or reversible), we use Chapter VIII, Equation (21):

$$c_p\,\mathrm{d}T + \mathrm{d}\phi = 0$$

$$\gamma_m = \frac{1}{c_p} \tag{11}$$

where $c_p \cong c_{p_d}(1 + 0.87\,r)$ (see Chapter IV, Equation (87)).

In the particular case when the air is dry, $r = 0$ and

$$\begin{aligned}\gamma_d = \frac{1}{c_{p_d}} &= \frac{1}{1005}\ \mathrm{kg\ K\ J^{-1}} \\ &= 0.009\,76\ \mathrm{K\ gpm^{-1}} \\ &= 9.76\ \mathrm{K\ gpkm^{-1}} \\ &= 0.003\,20\ \mathrm{K\ gpft^{-1}}.\end{aligned} \tag{12}$$

This process lapse rate is equal to the geometric lapse rate of a dry adiabatic atmosphere (cf. Chapter VIII, Section 7).

The lapse rate for moist air will differ only slightly from γ_d, and can be expressed:

$$\gamma_m = \frac{\gamma_d}{1 + 0.87\,r} \cong \gamma_d(1 - 0.87\,r). \tag{13}$$

In the case of a polytropic ascent, as considered in Chapter VII, Section 11, δq is not zero in (10), and (11) is no longer valid. By following the same procedure as above, we derive in that case for the polytropic lapse rate γ_p:

$$\gamma_p = \frac{1}{c_p}\left(1 - \frac{\delta q}{\mathrm{d}\phi}\right) = \frac{1}{c_p} - \frac{\lambda}{gU} \tag{14}$$

where λ and U have the same meanings as before. The second term becomes important only for extremely low rates of ascent ($U < 1\ \mathrm{cm\ s^{-1}}$).

The derivation of the lapse rate for saturated conditions is more laborious, and the result depends slightly on whether we assume a saturated reversible expansion (Chapter

VII, Section 8) or a pseudoadiabatic one (Chapter VII, Section 9). We shall begin with the first case. The starting point may be either Chapter VII, Equation (81), which expresses the condition $ds = 0$, or again

$$\delta q = dh - v\,dp = 0.$$

Both are equivalent, for the process is assumed to be reversible, and therefore $\delta q = T\,ds$. We shall have

$$\gamma_w = -\frac{dT}{d\phi} = \frac{1}{v}\frac{dT}{dp} = \frac{p}{RT}\frac{dT}{dp} \tag{15}$$

where $R = R_d(1 + 0.61 r_w)$. The expression for dT/dp to be introduced here is found from the equation describing the process. We write Chapter VII, Equation (81), developing the differentials:

$$\frac{c_{p_d} + c_w r_{t,w}}{T}\,dT - \frac{R_d}{p_d}\,dp_d + \frac{l_v}{T}\,dr_w + \frac{r_w}{T}\,dl_v - \frac{r_w l_v}{T^2}\,dT = 0. \tag{16}$$

We use now the substitutions

$$p = p_d + e_w \tag{17}$$

$$dp_d = dp - de_w \tag{18}$$

$$r_w = \frac{\varepsilon e_w}{p - e_w} \tag{19}$$

$$dr_w = \frac{\varepsilon\,de_w}{p - e_w} - \frac{\varepsilon e_w\,dp}{(p - e_w)^2} + \frac{\varepsilon e_w\,de_w}{(p - e_w)^2}$$

$$= \frac{\varepsilon + r_w}{p - e_w}\,de_w - \frac{\varepsilon e_w}{(p - e_w)^2}\,dp, \tag{20}$$

we divide Equation (16) by dp and we further substitute

$$\frac{de_w}{dp} = \frac{de_w}{dT}\frac{dT}{dp} \tag{21}$$

$$\frac{dl_v}{dp} = \frac{dl_v}{dT}\frac{dT}{dp}. \tag{22}$$

We then solve for dT/dp, obtaining finally:

$$\frac{dT}{dp} = \frac{\dfrac{R_d}{p - e_w} + \dfrac{\varepsilon l_v e_w}{T(p - e_w)^2}}{\dfrac{c_{p_d} + c_w r_{t,w}}{T} - \dfrac{l_v r_w}{T^2} + \dfrac{r_w}{T}\dfrac{dl_v}{dT} + \dfrac{de_w}{dT}\left[\dfrac{R_d}{p - e_w} + \dfrac{l_v(\varepsilon + r_w)}{T(p - e_w)}\right]}. \tag{23}$$

If we introduce this expression into expression (15), take into account the relation between R and R_d, Equations (12), (19), and the Kirchhoff and Clausius-Clapeyron equations:

$$\frac{dl_v}{dT} = c_{pv} - c_w \tag{24}$$

$$\frac{de_w}{dT} = \frac{l_v e_w}{R_v T^2} = \frac{\varepsilon l_v e_w}{R_d T^2} \tag{25}$$

we can obtain the expression

$$\gamma_w = \gamma_d \frac{\dfrac{p}{p - e_w}\left[1 + \left(\dfrac{l_v}{RT} - 0.61\right) r_w\right]}{1 + \dfrac{c_{pv} r_w + c_w (r_{t,w} - r_w)}{c_{pd}} + \dfrac{l_v^2 r_w (\varepsilon + r_w)}{c_{pd} R_d T^2}}. \tag{26}$$

This formula gives the lapse rate for the reversible saturated adiabatic expansion, and depends slightly on the proportion of liquid water referred to the unit mass of dry air $(r_{t,w} - r_w)$. The formula for the pseudoadiabatic process will be obtained from Equation (26) by setting $(r_{t,w} - r_w) = 0$, i.e., by suppressing in the denominator the term with c_w.

Equation (26) can be simplified by several approximations. In the numerator, $0.61 \ll l_v/RT$, so that the term 0.61 can be neglected. The ratio $p/(p - e_w)$ can differ by a few per cent from unity; it can be set equal to unity within that approximation. The second term in the denominator can also amount to a few per cent, and if we neglect it, the error will be partly compensated by the previous approximation. Finally $r_w \ll \varepsilon$ so that r_w can also be neglected in the last term of the denominator. The result of these simplifications is the formula

$$\gamma_w \cong \gamma_d \frac{1 + \dfrac{l_v r_w}{RT}}{1 + \dfrac{\varepsilon l_v^2 r_w}{c_{pd} R_d T^2}}. \tag{27}$$

And writing $r_w \cong \varepsilon e_w / p$, $R \cong R_d$,

$$\gamma_w \cong \gamma_d \frac{1 + \dfrac{\varepsilon l_v e_w}{R_d T p}}{1 + \dfrac{\varepsilon^2 l_v^2 e_w}{c_{pd} R_d T^2 p}}. \tag{28}$$

This approximate expression does not distinguish between the reversible and the pseudoadiabatic process. It might have been derived directly from the approximate

expression Chapter VII, Equation (83) with $c_p \cong c_{pd}$ by following a similar procedure to that leading to expression (26), introducing the same approximations as for the derivation of Equation (28) and making the additional simplification of neglecting unity against $\varepsilon l_v/R_d T \sim 20$.

We can illustrate the errors involved in these approximations by giving a numerical example. Let us assume that $T = 17\,^\circ\text{C}$, $p = 1000$ mb; thus $e_w = 19.4$ mb, $r_w = 0.0123$. Assuming that $r_{t,w} = 0.0163$ (corresponding to a large liquid water content of 4 g kg^{-1} of dry air), Equation (26) gives

$$(\gamma_w)_{rev} = 4.40 \text{ K gpkm}^{-1}.$$

Setting $r_{t,w} = r_w$ (no liquid water), Equation (26) gives for the pseudoadiabatic process:

$$(\gamma_w)_{ps} = 4.42 \text{ K gpkm}^{-1}$$

i.e., a value only 0.5% higher. The approximate formula (28) gives

$$\gamma_w \cong 4.53 \text{ K gpkm}^{-1}.$$

With numerical values of the constants, Equation (28) reads

$$\gamma_w \cong 9.76 \frac{1 + 5.42 \times 10^3 e_w/Tp}{1 + 8.39 \times 10^6 e_w/T^2 p} \text{ K gpkm}^{-1}. \tag{29}$$

Equation (26), or the approximate relations (28) or (29), permits the computation of γ_w as a function of T and p. The second term in the numerator of Equation (28) is always smaller than the second term in the denominator (because $\varepsilon < l_v/c_{pd} T = 2500/T$ in the atmosphere), and therefore $\gamma_w < \gamma_d$. The largest differences are found for high values of T (and therefore high values of e_w), when γ_w decreases to near 3 K gpkm^{-1}. For lower T, e_w decreases rapidly and, unless p is also very low, the second terms in the numerator and denominator become negligible, so that γ_w tends to the value $\gamma_d = 9.76$ K gpkm^{-1}. In an aerological diagram this means that for decreasing temperatures the saturated adiabats tend to coincide with dry adiabats of the same pseudo-equivalent potential temperature θ_{ae}.

The previous derivations refer to water clouds. The same formulas hold for ice clouds, provided we make the corresponding substitutions: l_s, e_i and r_i for l_v, e_w and r_w.

9.4. The Lapse Rates of the Parcel and of the Environment

Let us go back now to the stability criteria (9) and consider the virtual temperature lapse rates γ'_v and γ_v.

According to the initial assumptions, the virtual processes undergone by the parcel must be adiabatic. If the parcel is not saturated, as there is no mixing with the surroundings, the mixing ratio r_0 will be a constant, and the process is a moist adiabatic expansion (or compression). By differentiating

$$T'_v = (1 + 0.61 r_0) T' \tag{30}$$

with respect to ϕ and changing sign, we obtain:

$$\gamma'_v = (1 + 0.61\, r_0)\gamma_m = (1 + 0.61\, r_0)(1 - 0.87 r_0)\gamma_d = (1 - 0.26 r_0)\gamma_d \quad (31)$$

where γ_m is the lapse rate for the moist adiabat and γ_d that for the dry adiabat.

The term $0.26\, r_0$ is small compared with unity and therefore we may neglect it as a first approximation. Thus

$$\gamma'_v \cong \gamma_d \quad (\textit{unsaturated parcel}). \quad (32)$$

If on the other hand the parcel is saturated, its mixing ratio r_w must decrease during the ascent. By proceeding as before, we have:

$$T'_v = (1 + 0.61\, r'_w)T' \quad (33)$$

$$\gamma'_v = (1 + 0.61\, r'_w)\gamma_w - 0.61\, T' \frac{dr'_w}{d\phi} \quad (34)$$

where γ_w is the saturated adiabatic lapse rate.

We remark now that $dr'_w/d\phi < 0$, $\gamma'_v > \gamma_w$, and as r'_w and its derivative decrease with ascent, γ'_v becomes closer to γ_w. For the lower troposphere the last term may amount to as much as 10% of γ_w; if we neglect this term as a first approximation, as well as $0.61\, r_w$ against unity,

$$\gamma'_v \cong \gamma_w \quad (\textit{saturated parcel}). \quad (35)$$

Therefore, we identify the lapse rate of the parcel approximately with γ_d or γ_w, according to whether it is unsaturated or saturated. In Section 3 we have derived the values for these two quantities.

We may now consider the lapse rate of the environment in a similar way, but remembering that here we are dealing with a geometric derivative rather than with a physical process. We shall have

$$T_v = (1 + 0.61\, r)T \quad (36)$$

$$\gamma_v = (1 + 0.61\, r)\gamma - 0.61\, T \frac{\delta r}{\delta \phi}. \quad (37)$$

If we take into account the relation (9), the last term indicates that according to whether $\delta r/\delta\phi \gtrless 0$, the humidity distribution with height will increase or decrease the vertical stability. In certain conditions this term may become quite appreciable. Let us consider an example. We assume $\gamma = 0$, for simplicity. Now we ask what distribution or r may determine a value $\gamma_v = l/c_{p_d} = \gamma_d$ for the lapse rate. It will be:

$$\frac{\delta r}{\delta \phi} = -\frac{\gamma_d}{0.61\, T} \cong -6 \times 10^{-5}\ \text{gpm}^{-1}.$$

This condition would be satisfied, for instance, if the mixing ratio decreased by

8.6×10^{-3} along 150 gpm. This variation could be present in a layer whose base was saturated at 10 °C and 900 mb and whose top was dry. Such vertical humidity gradients could arise in the case of dry inversion layers above cloud strata.

We may also define a potential temperature lapse rate and derive its value for an unsaturated atmosphere as a function of the lapse rate γ_v. If we differentiate logarithmically the definition of θ_v:

$$\theta_v = T_v\left(\frac{1000}{p}\right)^{\varkappa_d} \quad (p \text{ in mb}), \tag{38}$$

we obtain

$$\frac{1}{\theta_v}\frac{\delta\theta_v}{\delta\phi} = \frac{1}{T_v}\frac{\delta T_v}{\delta\phi} - \frac{\varkappa_d}{p}\frac{\delta p}{\delta\phi}. \tag{39}$$

If we now introduce Chapter VIII, Equation (21), the definition of $\varkappa_d$, the gas law and the value of γ_d, we obtain

$$\frac{\delta\theta_v}{\delta\phi} = \frac{\theta_v}{T_v}(\gamma_d - \gamma_v) \tag{40}$$

which gives, except for the sign, the lapse rate of θ_v. This is therefore proportional to the difference between γ_v and the adiabatic lapse rate. If $\gamma_v = \gamma_d$, we have $\theta_v = \text{const.}$ (adiabatic atmosphere).

9.5. Stability Criteria for Adiabatic Processes

Within the approximations made in the previous paragraph, we may now write the criteria (9) in the following form:

$$\gamma_v \gtrless \gamma_d \quad \textit{unsaturated parcel}, \tag{41}$$

$$\gamma_v \gtrless \gamma_w \quad \textit{saturated parcel}, \tag{42}$$

where, as before, the sign $>$ corresponds to *instability*, the sign $=$ to *indifference*, and the sign $<$ to *stability*.

We have here relations between thermal gradients, that is between derivatives of the temperature with respect to ϕ. The geopotential is proportional to the height z, and the variables $-p$, $-\ln p$ or $-p^{\varkappa}$ increase monotonically with z. Therefore, the relative values of the derivatives T with respect to these variables will follow the same order as the lapse rates γ. In the diagrams (tephigram, emagram, Stüve) where T is the abscissa, the curves giving the variation of T will appear more inclined backwards the higher the value of γ. For any of these representations we may thus visualize the conditions (41) and (42) by means of the diagram shown in Figure IX-3.

The procedure consists in observing, for a point P_0 of the state curve, what relation the slope of the curve bears to the slopes of the dry and saturated adiabats. According to the slope, the curve will fall within one of the stability regions; thus

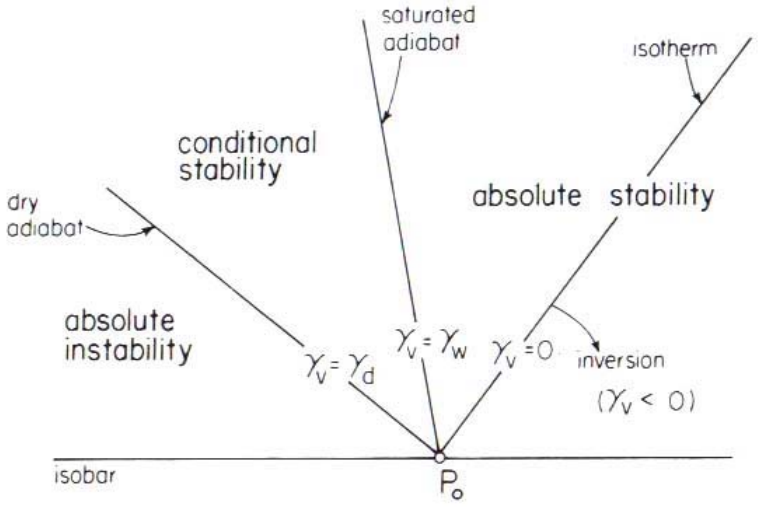

Fig. IX-3. Lapse-rate regions of stability, on a diagram.

the zone of absolute instability corresponds to $\gamma_v > \gamma_d$

the zone of conditional instability corresponds to $\gamma_w < \gamma_v < \gamma_d$

the zone of absolute stability corresponds to $\gamma_v < \gamma_w$

The word 'absolute' indicates that the stability or instability condition holds independently of the air saturation. The designation of "conditional instability" means that, if the air is saturated, there will be instability ($\gamma_v' \cong \gamma_w < \gamma_v$), and in the opposite case, there will be stability ($\gamma_v' \cong \gamma_d > \gamma_v$).

Let us consider now an unsaturated parcel in the case of instability. We shall have $\gamma_v > \gamma_d$, and in a diagram the state curve (γ_v) and the process curves (γ_d) will appear as in Figure IX-4, where θ, θ', θ'', θ''' indicate dry adiabats of decreasing potential temperatures. It is obvious that for rising ϕ, the state curve cuts dry adiabats of

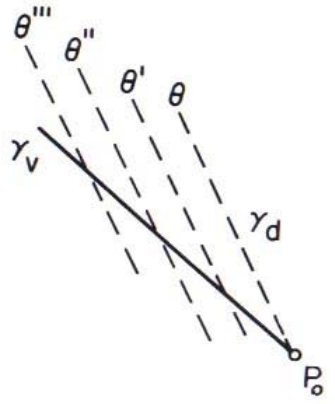

Fig. IX-4. Potential temperature decrease with height for a superadiabatic lapse rate.

decreasing potential temperature θ; that is, $\delta\theta_v/\delta\phi<0$. If we had started with the stability case, we would have arrived at the opposite result. On the other hand, the argument may be applied in a similar way to the case of a saturated parcel, if instead of γ_d we consider the lapse rate γ_w, and we substitute the potential wet bulb temperature θ_{aw} or the potential equivalent temperature θ_{ae} for θ, these temperatures being the

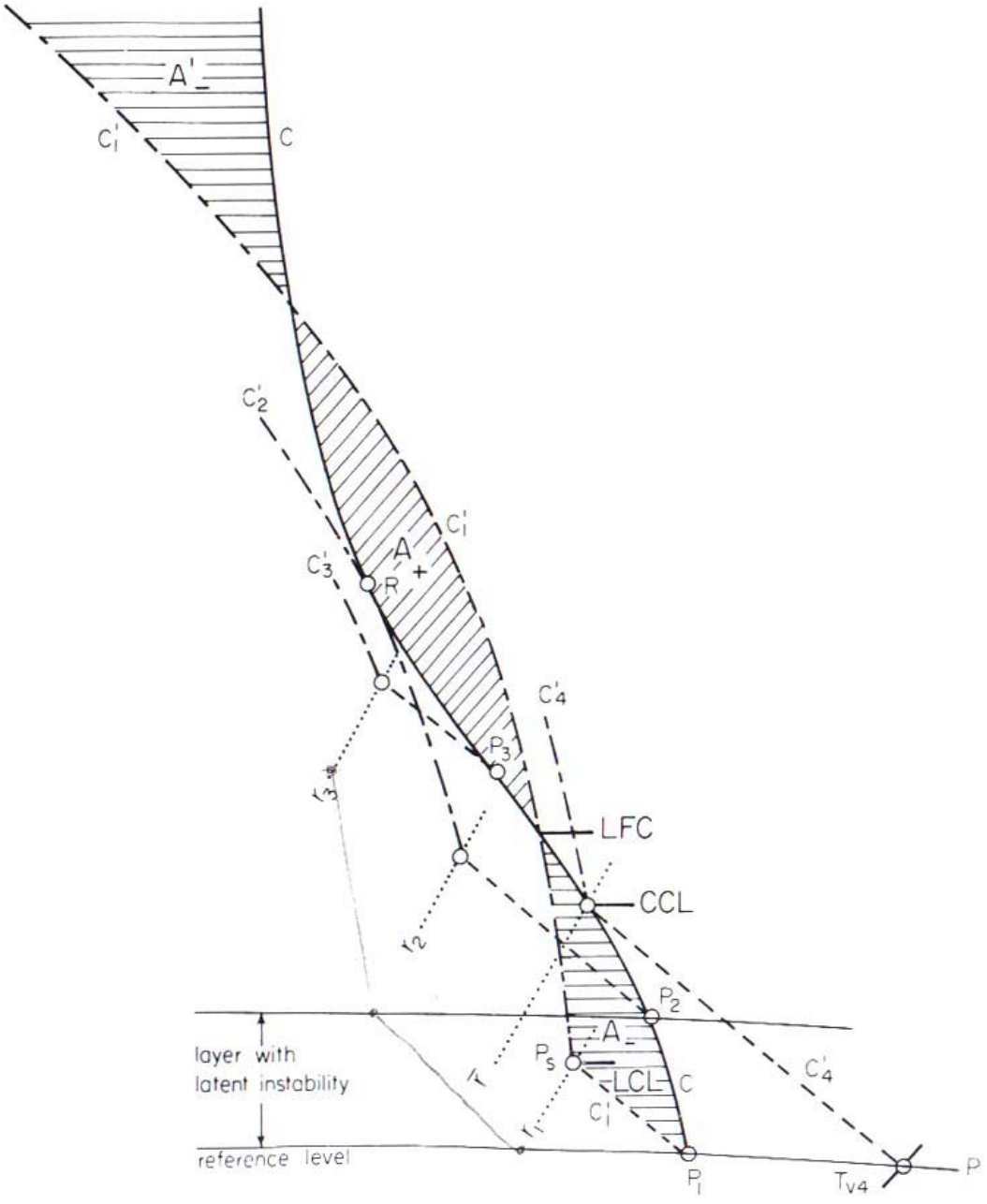

Fig. IX-5. Latent instability.

invariants characteristic of the saturated adiabats. We may therefore express the stability conditions in the following alternative way:

$$\frac{\delta\theta_v}{\delta\phi} \lessgtr 0 \qquad \textit{unsaturated parcel} \tag{43}$$

$$\frac{\delta\theta_{aw}}{\delta\phi} \lessgtr 0 \quad \text{or} \quad \frac{\delta\theta_{ae}}{\delta\phi} \lessgtr 0 \qquad \textit{saturated parcel} \tag{44}$$

where now the sign $<$ corresponds to *instability*, the sign $=$ to *indifference*, and the sign $>$ to *stability*. Obviously the same conditions can be written with the z derivatives, instead of using the geopotential.

The relation (43) could also have been derived by introducing Equation (41) in (40).

9.6. Conditional Instability

In Section 5 we have denoted by conditional instability the case $\gamma_w < \gamma_v < \gamma_d$. All arguments so far have been based on infinitesimal virtual displacements. They have been used therefore to analyze the stability conditions at a certain point or, as we are studying an atmosphere where all properties are constant on equipotential surfaces, at a given level.

We shall now study the stability conditions in a conditionally unstable layer, such as that extending from the surface (P_1) to the point R of the state curve in Figure IX-5 (representing a tephigram). All the points of the state curve within that layer obey the conditional instability criterion. But we shall now discuss what happens when parcels coming from different levels rise along the vertical, in finite displacements.

The temperature distribution of the atmosphere is represented by the curve c (sounding). The curves c'_1, c'_2 and c'_3 represent the processes undergone by parcels coming from the reference levels P'_1, P'_2 and P'_3, respectively.

When a parcel rises vertically in the atmosphere, a certain amount of work is performed by or against the buoyancy forces according to whether the process curve lies at the right or at the left of the state curve. We shall now show that this work is proportional to the area enclosed between the two curves and the isobars defining the initial and final levels, in any area-preserving diagram.

Let us first consider the process on an emagram (Figure IX-6). The work done by the buoyant force on the parcel, per unit mass, will be

$$w = \int_a^b \ddot{z}\, dz, \tag{45}$$

and taking into account Equation (4), (Chapter VIII, Equation (21)) and the gas law,

$$w = g\int_a^b \frac{v' - v}{v}\,dz = -\int_a^b (v' - v)\,dp$$

$$= R_d\int_a^b (T_v' - T_v)\,d(-\ln p)$$

$$= R_d(\Sigma'_{em} - \Sigma_{em}), \tag{46}$$

where Σ'_{em} and Σ_{em} are the areas defined by the two isobars, the vertical axis, and the curve c' or c, respectively. The difference is the area shaded in the figure. This is a closed area which might be considered as the representation of a cycle. We have seen in Chapter VI that the same cycle will define a proportional area in any other area-preserving diagram, such as, for instance, the tephigram.

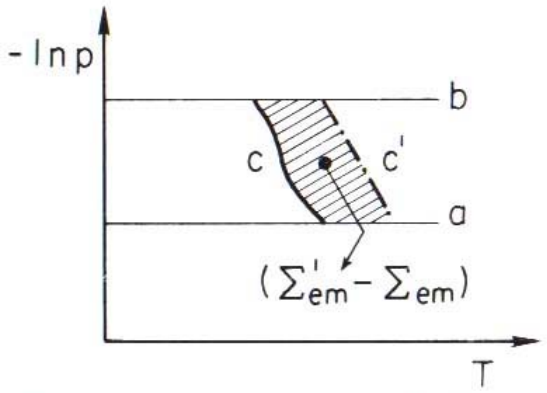

Fig. IX-6. Work performed on a parcel by buoyancy.

Let us go back now to the process that we are considering. The work received per unit mass of the parcel will be transformed into kinetic energy:

$$w = \int_a^b \ddot{z}\,dz = \int_a^b \frac{d\dot{z}}{dt}\,dz = \int_a^b \dot{z}\,d\dot{z} = \tfrac{1}{2}(\dot{z}_b^2 - \dot{z}_a^2), \tag{47}$$

where $\frac{1}{2}\dot{z}^2$ is the kinetic energy of the unit mass. If c' is to the right of c, as in the figure, w is positive: work is done on the parcel by the external forces of gravity and pressure, and the parcel accelerates. If c' is to the left of c, w is negative and the parcel decelerates; in order to rise, the parcel must be provided with an energy equal to the negative area that it determines on the diagram along the ascent.

In Figure IX-5, in order for the parcel to follow the path c'_1, work proportional to the area A_- must be performed against the negative buoyant force (for instance, the necessary energy could come from a forced orographic ascent). The level at which it reaches saturation (point P_s) is called the *lifting condensation level* (LCL).

When the parcel surpasses the level at which the process curve crosses the state

curve, the buoyant force performs a work proportional to the area A_+, up to the isobar reached. Convection will thus continue freely until c_1' crosses again c, and the parcel decelerates. The level of the first crossing is called the *level of free convection* (LFC). The total area A_+ measures the *latent instability* for a parcel at the reference level P_1.

One can proceed similarly with parcels from other levels. When the level of P_2 is reached, A_+ vanishes: this is the upper limit of the layer for which there is latent instability. For instance, c_3' does not show any latent instability.

It may be noticed that the instability is greater for higher T and r. When r increases, the segment P_1P_s becomes shorter, A_- decreases and A_+ increases. Regarding the temperature, if we assume that after the sounding c, the ground is warmed up by radiation (insolation), a steeper lapse rate γ_v will appear in the lowest layer; when it exceeds the dry adiabatic lapse γ_d, the layer becomes unstable and a vertical mixing process starts working, which results in a dry adiabatic lapse rate for that layer (cf. Chapter VII, Section 12). As the warming continues, an increasing depth of the lowest part of the sounding becomes substituted by dry adiabats of increasing potential temperature. Eventually, the top of the stirred layer may reach saturation, that is, the dry adiabatic portion c_4' reaches the mixing ratio isopleth corresponding to the mean value for the layer $\bar{r}$. This level is called the *convective condensation level* (CCL). The temperature of the ground has reached then the value T_{v_4} (see Figure IX-5) and from that moment, convection may proceed spontaneously (along c_4', dry adiabat up to CCL and then saturated adiabat) without any need of forced lifting.

We have mentioned that in Figure IX-5 the lower part of the sounding has been assumed to have lapse rates between γ_d and γ_w, corresponding to conditional instability. Conditional instability is sometimes classified into three types:

Conditional instability	of the real *latent type*:	when $A_+ > A_-$, as in Figure IX-5.
	of the *pseudolatent type*:	when $A_+ < A_-$.
	of the *stable* type:	when no positive area A_+ appears for parcels of any level.

Because a measure of the instability area can take too long for routine application, it is frequently substituted by the determination of the difference of temperature $T_v - T_v'$ at 500 mb for parcels rising from the 850 mb level; this value is called the *Showalter stability index*. The larger positive this index is, the greater is the local stability. Large negative areas, on the other hand, will correspond to large negative values (i.e., several degrees) of the index.

It must be kept in mind that this analysis of vertical stability must be assessed in the context of the synoptic situation and taking into account the approximations involved. For instance, the difference of areas $A_+ - A_-$ may not be particularly important if A_- is large enough to prevent the onsetting of convection. Conversely, small negative areas may easily be eliminated during insolation or may not even be meaningful, in view of the local temperatures' contrasts, which are not taken into account in the analysis; these differences will exist owing to the different characteristics of the ground surface (low heat

capacity and conductivity of the ground will favor overheating of its surface) and convection (updrafts or thermals) will start over the areas at higher temperature.

9.7. Oscillations in a Stable Layer

If some disturbance provokes a vertical displacement in a stable layer ($\gamma_v' < \gamma_v$), an oscillatory motion results. This will actually be damped by turbulent mixing of the borders of the parcel with the environment. For the parcel method, which does not take into account this effect, the motion will be undamped.

The acceleration is (formula (8)):

$$\ddot{z} = -\frac{g^2}{T_v}(\gamma_v' - \gamma_v) z \tag{48}$$

where z is now written for the displacement. This is the equation for the motion of a linear harmonic oscillator:

$$\ddot{z} + kz = 0, \tag{49}$$

where the force constant is

$$k = \frac{g^2}{T_v}(\gamma_v' - \gamma_v) = \omega^2 = \left(\frac{2\pi}{\tau}\right)^2 \tag{50}$$

(ω = angular frequency; τ = period). The solution is

$$z = A \sin \omega t, \tag{51}$$

and the period

$$\tau = \frac{2\pi}{g}\sqrt{\frac{T_v}{\gamma_v' - \gamma_v}} \tag{52}$$

will be larger, the smaller the difference between the lapse rate of parcel and environment. The angular frequency of such (gravity) waves is usually referred to as the Brunt-Vaisala frequency.

For example, let us assume that

$$T_v = 0\,^\circ\mathrm{C}, \qquad \gamma_v = 0, \qquad \gamma_v' \cong \gamma_d = 1/c_{p_d} \quad \text{(unsaturated parcel)}.$$

We obtain:

$$\tau = 335 \text{ s} = 5.6 \text{ min}$$

If $A = 200$ m, the maximum velocity of the oscillation will be

$$\dot{z}_{max} = A\omega = \frac{200 \times 2\pi}{335} = 3.7 \text{ m s}^{-1}.$$

9.8. The Layer Method for Analyzing Stability

As we remarked in Section 1, one of the main defects of the parcel method is the assumption that the environment remains undisturbed. The ascent of an air mass must necessarily be compensated by the descent of surrounding air. If the rising masses cover an appreciable fraction of the total area, the error becomes important. In order to allow for the compensatory descending motion, Bjerknes devised the layer, or 'slice', method, which we shall describe now.

Let us consider a certain level, over an area large enough to cover a representative number of possible ascending currents (Figure IX-7). Let us discuss a virtual process by which updraughts start, covering an area A', while this movement is compensated

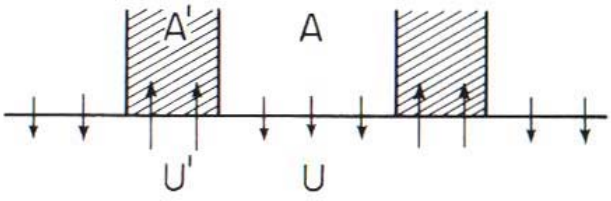

Fig. IX-7. Ascending and descending motions according to the layer method.

by a general descent of the environment, covering an area A. We assume that the velocities are constant and equal to U' (upwards) and U (downwards). The layer is initially uniform. The total mass of ascending and descending air must be equal:

$$A'U' = AU\,. \tag{53}$$

For a time interval dt, the displacements of ascending and descending air will be dz' and dz, respectively, and

$$\frac{U}{U'} = \frac{dz/dt}{dz'/dt} = \frac{dz}{dz'} = \frac{A'}{A} \tag{54}$$

where the velocities and displacements are expressed as absolute values.

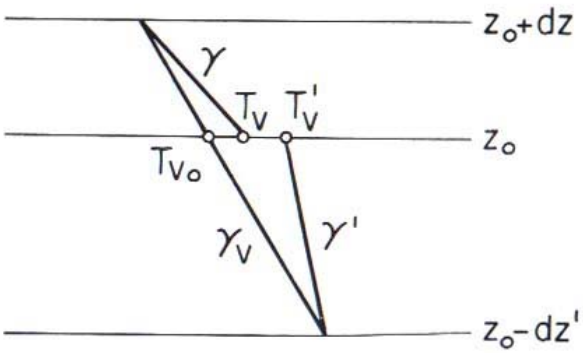

Fig. IX-8. Layer method. Case $\gamma_w < \gamma_v < \gamma_d$ with instability.

The stability conditions will result, as in the parcel method, from the value of the acceleration $\ddot{z}$ of the rising air as given by Equation (4). In order to calculate the difference $(T'_v - T_v)$, we shall consider the level z_0 of the layer at the time dt of the virtual displacement. The air crossing z_0 upwards comes from the level $z_0 - dz'$, and the air crossing downwards, from $z_0 + \mathrm{d}z$ (Figure IX-8). γ_v, γ' and γ are, respectively, the geometric lapse rate of the atmosphere at z_0 (at the initial time), and the process lapse rate (for virtual temperature, although the subscript v has been dropped here for convenience) of ascending and descending air (approximately γ_d or γ_w, as the case may be, according to Section 4). If the initial (virtual) temperature at z_0 is T_{v_0}, at the time dt we shall have, for the temperatures of the ascending and descending air:

$$
\begin{aligned}
T'_v &= T_{v_0} + \gamma_v g\, \mathrm{d}z' - \gamma' g\, \mathrm{d}z' = T_{v_0} + (\gamma_v - \gamma') g\, \mathrm{d}z' \\
T_v &= T_{v_0} - \gamma_v g\, \mathrm{d}z + \gamma g\, \mathrm{d}z = T_{v_0} + (\gamma - \gamma_v) g\, \mathrm{d}z \\
\Delta T_v &= T'_v - T_v = (\gamma_v - \gamma') g\, \mathrm{d}z' - (\gamma - \gamma_v) g\, \mathrm{d}z \\
&= g \left[(\gamma_v - \gamma') - \frac{A'}{A} (\gamma - \gamma_v) \right] \mathrm{d}z' \qquad (55)
\end{aligned}
$$

where the relation (54) has been introduced. Replacing ΔT_v in Equation (4) by (55), we have for the rising air:

$$
\ddot{z} = \frac{g^2}{T_v} \left[(\gamma_v - \gamma') - \frac{A'}{A} (\gamma - \gamma_v) \right] \mathrm{d}z' ,
$$

and arguing as in Section 2, we obtain as the stability criterion, that in the relation

$$
(\gamma_v - \gamma') - \frac{A'}{A} (\gamma - \gamma_v) \gtrless 0 \qquad (56)
$$

the sign $>$ corresponds to *instability*, the sign $=$ to *indifference*, and the sign $<$ to *stability*.

It may be noticed that for the particular case in which the area of rising air is a negligible fraction of the total area, $A'/A \cong 0$, and Equation (56) becomes equal to the conditions (9) derived with the parcel method.

Let us consider now the different possible cases.

(I) $\gamma_w < \gamma_v < \gamma_d$ (conditional instability) and the air is saturated at the level z_0. It is the case of a layer at the condensation level. The rising saturated air will follow a saturated adiabat, while the descending air will follow a moist (approximately a dry) adiabat: $\gamma' \cong \gamma_w$ and $\gamma \cong \gamma_d$. Condition (56) becomes

$$
\frac{\gamma_v - \gamma_w}{\gamma_d - \gamma_v} \gtrless \frac{A'}{A} = \frac{U}{U'} \qquad (57)
$$

where the upper sign corresponds always to instability. Stability does not depend only on the value of γ_v, but also on the relative extent of convection. Instability will be

reached more easily if this extent is small (i.e., small $A'/A = U/U'$). Figure IX-8 corresponds to instability, and Figure IX-9 to stability.

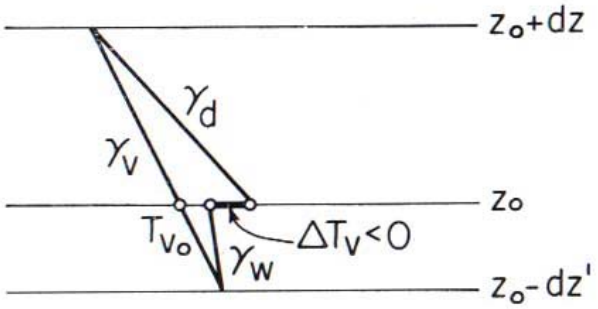

Fig. IX-9. Layer method. Case $\gamma_w < \gamma_v < \gamma_d$ with stability.

(II) $\gamma_v > \gamma, \gamma'$. Whatever may be the values of γ, γ' and A'/A, Equation (56) indicates instability, because both terms on the left side are positive. Let us notice that, according to this method, ΔT_v is larger than for the parcel method, which only gives the first term of Equation (55).

This may be the case of unsaturated air rising in an unsaturated environment ($\gamma = \gamma' = \gamma_d$), of saturated air in a saturated environment ($\gamma = \gamma' = \gamma_w$), or of saturated air rising in an unsaturated environment ($\gamma = \gamma_d$; $\gamma' = \gamma_w$); in the last case the reference level is the saturation level.

These cases are shown by Figure IX-10.

(III) $\gamma_v < \gamma, \gamma'$. Whatever may be the values of γ, γ' and A'/A, Equation (56) indicates stability, because both terms on the left are negative. Again the difference ΔT_v (negative) is larger in absolute value than in the parcel method.

Figure IX-11 corresponds to this case, for which we have the same possibilities as in (II) regarding saturation.

Thus, the layer method shows us that the effect of the environment subsidence due to the convection is as follows: when the parcel method indicates absolute instability, this effect makes the instability even more pronounced; when there is absolute stability, it makes it even more stable; when there is conditional instability, the environment

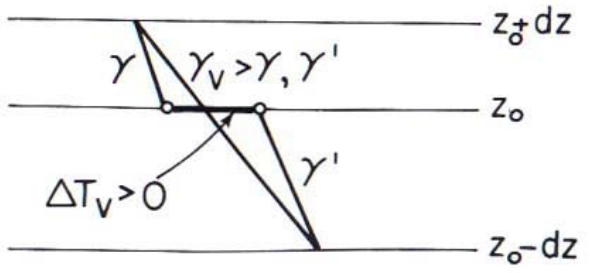

Fig. IX-10. Layer method. Case $\gamma_v > \gamma, \gamma'$ (absolute instability).

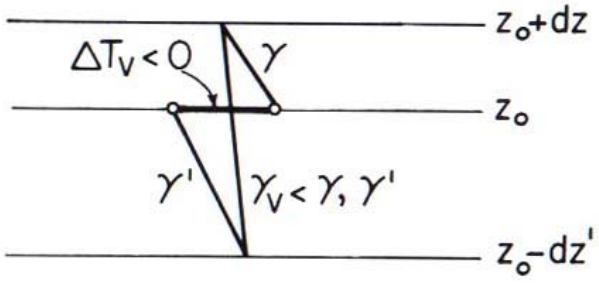

Fig. IX-11. Layer method. Case $\gamma_v < \gamma, \gamma'$ (absolute stability).

subsidence qualifies it in such a way that the instability becomes less pronounced and may even revert to stability, according to the extent of the convection and to the particular value of γ_v.

The layer method constitutes an improvement over the parcel method in that it disposes of one of its most objectionable assumptions. It provides a satisfactory tool for the analysis of stability at a given level by considering infinitesimal virtual motions. Its application, however, requires an estimate of the parameter A'/A, and this would generally be an arbitrary guess.

9.9. Entrainment

When the parcel method is applied to finite vertical displacements, as in the analysis of conditional instability (Section 6), the assumption of no mixing with the surroundings remains as the main source of error; in fact, turbulent mixing is very active, and ignoring it is the cause of obtaining exaggerated values for the temperature difference between parcel and environment, the kinetic energy acquired by a saturated parcel and its liquid water content. The main effect of mixing is to incorporate into the rising parcel a certain amount of external air that becomes mixed with the rest of the parcel; this is called 'entrainment'. There is also the possibility of 'detrainment', i.e., of a certain proportion of the rising parcel being shed and coming to a halt while mixing with the surrounding air. If we take into account only the first effect and an estimate can be made for the proportion of external air being entrained per unit length of ascent (rate of entrainment), a convenient correction of the parcel method predictions can be worked out. This will now be explained. The rate of entrainment, however, is a highly variable parameter, depending on the stage of development of the cloud, the dimensions of the ascending mass and the intensity of the convection (vertical velocities), therefore difficult to estimate, but the method will show how the effect of entrainment on convective parameters can be visualized by a simple graphical procedure on a diagram.

We divide the ascent into a number of steps, and consider each step as consisting of three processes:

(a) the air rises Δz, without mixing, as in the parcel method;

(b) it mixes isobarically with a certain proportion of the surrounding air (cf. Chapter VII, Section 4); and

(c) liquid water from the parcel evaporates, until the gaseous phase becomes again saturated (adiabatic isobaric evaporation), or until the water has completely evaporated. This process will not be required if the parcel is not saturated before or after mixing.

By repeating this procedure in successive steps, a much more realistic curve can be obtained for the rising parcel properties whenever we can have a reasonable estimation of the proportion of external air incorporated in each step.

The correction could be computed from the formulas in Chapter VII, but it is more conveniently estimated on a diagram. Let us consider Figure IX-12, where one step

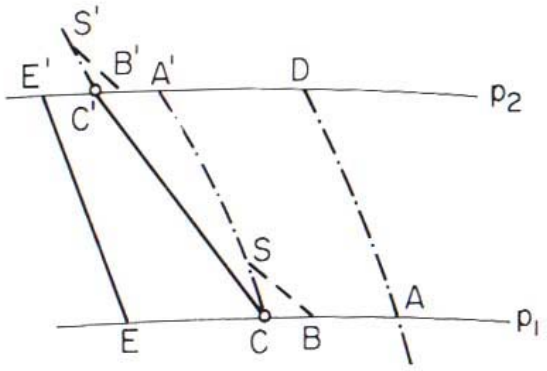

Fig. IX-12. Graphical correction for entrainment.

of the process is followed on a tephigram. We assume that EE' is the state curve of the environment, AD the saturated adiabat that the parcel would follow if it ascended without mixing from the point A (reached from a previous step, process (a)). We shall assume that in every step 50% of external air is incorporated (and no air from the parcel is lost). At the level p_1 isobaric mixing takes place (process (b)); the point B results from mixing air masses E and A in the assumed proportions. According to the rule of mixtures, the segment BA will be in our example one-third of EA, because the resulting temperature must be the weighted average of T_E and T_A. Process (c) is substituted with sufficient approximation by the process defining the pseudo-wet-bulb temperature (Chapter VII, Section 13): ascent along the dry adiabat until saturation (point S), and descent along the saturated adiabat to level p_1. We obtain thus point C, representing the parcel at level p_1.

A new ascent to the next step will bring the parcel to A' at level p_2, where the processes of mixing and evaporation are performed again in a similar way. Point C' is then obtained. The segment CC' is the corrected trajectory of the parcel between the levels p_1 and p_2. By repeating the procedure, new segments will be added, and the whole curve, between the convective condensation level and the level at which all the liquid water disappears after crossing the state curve to the left, can be constructed.

It will be remarked that in each step the resulting humidity of the isobaric mixture

has to be computed analytically in order to be able to determine the saturation point S.

Entrainment can have a major effect on cumulus convection processes, and in particular on their evolution in time. If the environment air surrounding the cumulus cloud is relatively dry, as it will be during the early stages of the growth of the cloud, detrainment (or external entrainment) will result in dissolution of cloud elements, leaving, however, a moister environment than previously existed. The temperature of the rising air will decrease as a result of the initial mixing and of the subsequent evaporation, reducing or even nullifying the relative buoyancy of the rising parcel. The same process will cause isolated cloud turrets to dissolve and appear to fall back into the parent cloud. Internal entrainment will similarly reduce the liquid water content and buoyancy of cloud elements inside the cloud, so that the net effect of these processes is to produce horizontal gradients of liquid water content and vertical velocities, with maximum values in the interior of the cloud. Only in the central core of a cumulus cloud can one achieve theoretical values of liquid water content (usually known as 'full adiabatic' values). Vertical velocities, even at the core, seldom reach their theoretical values because of the reduction of cloud buoyancy, and as a result cumulus cloud tops seldom reach the predicted level (of equilibrium with the environment). A further consequence of these mixing processes is that the cloud soon develops a dome shape, rather than a cylindrical shape. If an ample supply of energy exists, the damping effect of the environment will decrease as its relative humidity increases, until eventually a more-nearly columnar development of the cloud to high levels is possible and the cumulus cloud becomes a cumulus congestus.

9.10. Potential or Convective Instability

With the parcel method, we have so far considered the stability properties of the atmosphere when an isolated mass, the parcel, is vertically displaced. This occurs, for instance, when the warming of the lower layers causes the ascent of air masses with dimensions of the order of hundreds of meters to 1 km. These masses can eventually become accelerated by a latent instability, as we have seen. They are called *thermals* or *bubbles*, and become visible as convective clouds. When the convection becomes more intense we may have, instead of isolated masses, a continuous jet of ascending air. The previous calculations would apply equally to this type of convection.

It is also important to study the vertical movements of an extended layer of atmosphere, such as may occur, for instance, during the forced ascent of an air mass over an orographic obstacle, or due to large-scale vertical motions of appreciable magnitude (as, for example, in frontal situations). We shall now consider this case, deriving the effect of the movement on the lapse rate of the layer.

9.10.1. The layer is and remains non-saturated

We represent the layer δz in Figure IX-13, where the right hand side is a diagram z, T (the relations would be similar on a tephigram). This layer ascends from p to p'; at the first level the area considered will be A' and the thickness $\delta z'$. The virtual

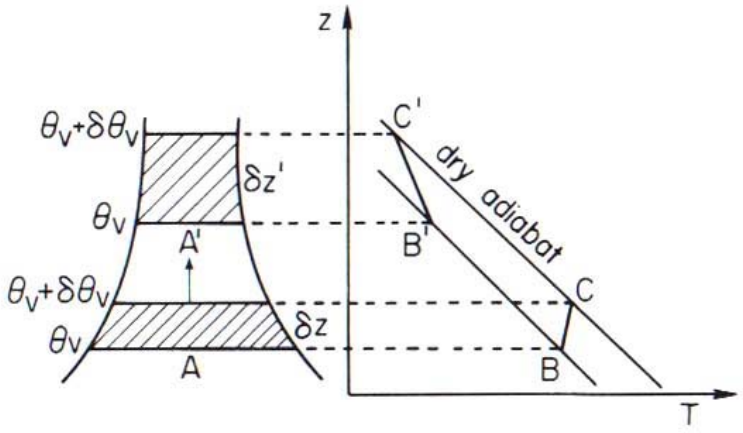

Fig. IX-13. Potential instability, non-saturated layer.

potential temperature θ_v of the base of the layer will remain constant during the ascent, which we assume adiabatic, and the same will happen with the temperature $\theta_v+\delta\theta_v$ of the top of the layer; therefore the variation $\delta\theta_v$ through the layer also remains constant.

Conservation of the total layer mass requires that

$$\varrho A\,\delta z = \varrho'\,A'\,\delta z' \tag{58}$$

or

$$\frac{\delta z'}{\delta z} = \frac{\varrho A}{\varrho' A'} = \frac{pAT_v'}{p'A'T_v} \tag{59}$$

where all the primed variables correspond to the final state, the gas law having been introduced in the last expression.

As $\delta\theta_v$ remains constant, the gradient of θ_v must be inversely proportional to δz. We must have:

$$\frac{\delta\theta_v}{\delta z} = \frac{\delta\theta_v}{\delta z'}\frac{\delta z'}{\delta z} = \frac{\delta\theta_v}{\delta z'}\frac{pAT_v'}{p'A'T_v}. \tag{60}$$

Or, dividing both sides by g:

$$\frac{\delta\theta_v}{\delta\phi} = \frac{\delta\theta_v}{\delta\phi'}\frac{pAT_v'}{p'A'T_v}, \tag{61}$$

and introducing Equation (40):

$$\frac{\theta_v}{T_v}(\gamma_d - \gamma_v) = \frac{\theta_v}{T_v'}(\gamma_d - \gamma_v')\frac{pAT_v'}{p'A'T_v} \tag{62}$$

and solving for γ_v':

$$\gamma'_v = \gamma_d - \frac{p'A'}{pA}(\gamma_d - \gamma_v)$$

$$= \gamma_v + (\gamma_d - \gamma_v)\left(1 - \frac{p'A'}{pA}\right). \tag{63}$$

If $\gamma_v = \gamma_d$, $\gamma'_v = \gamma_d = \gamma_v$; that is, the layer is adiabatic and the ascent occurs along the same adiabat.

If $\gamma_v < \gamma_d$ (the usual case), both the vertical stretching (horizontal convergence; shrinking of the column: $A'/A < 1$) and ascending motion ($p'/p < 1$) increase the lapse rate, the layer thus becoming less stable. (This is the case of Figure IX-13.) Conversely, both the broadening of the layer (horizontal divergence: $A'/A > 1$) and the descending motion ($p'/p > 1$) decrease the lapse rate and therefore tend to stabilize the layer (this case is the opposite of Figure IX-13, but it can be visualized on the same figure by exchanging primed and unprimed letters).

If $\gamma_v > \gamma_d$, we would have the opposite effects, but this situation does not occur in the atmosphere, as it corresponds to absolute instability.

Equation (63) indicates that, for increasing $p'A'/pA$, the sign of the lapse rate can change, resulting in more or less pronounced inversions ($\gamma'_v < 0$). If on the contrary $p'A'/pA$ decreases tending to zero, γ'_v will tend to the dry adiabatic lapse rate γ_d.

These cases occur in large scale cyclones and anticyclones. In anticyclones, the subsidence frequently gives rise to inversions. In cyclones, the convergence aloft may lead to nearly-adiabatic lapse rates.

In the example of Figure IX-13, both effects (rising motion and shrinking) tend to make the layer more unstable, which becomes apparent by the increase in lapse rate from BC to $B'C'$.

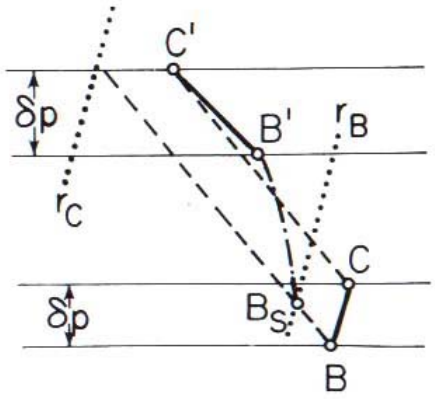

Fig. IX-14. Potentially unstable layer becoming partly saturated.

9.10.2. Part of the layer becomes saturated during the ascent

We shall not study this case analytically, but it is easy to see the qualitative effects on a diagram.

If we assume that $\delta\theta_{aw}/\delta z < 0$, i.e., that the layer is more humid at the base than at the top, the base will become saturated (BB_s) before the top in a rising motion. From that moment it will follow the saturated adiabat (B_sB'), while the top continues along a dry adiabat (CC'). This is shown schematically on a tephigram in Figure IX-14, where it is easy to see that the ascent makes the layer absolutely unstable. This is expressed by saying that the layer was originally *potentially unstable.*

If, on the contrary, $\delta\theta_{aw}/\delta z > 0$, we have the opposite effect, as shown in Figure IX-15, and the layer is said to be *potentially stable.*

If $\delta\theta_{aw}/\delta z = 0$, the layer is said to be potentially neutral.*

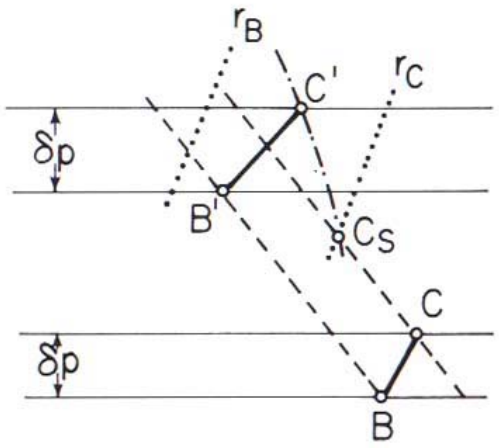

Fig. IX-15. Potentially stable layer becoming partly saturated.

In the case of bulk ascent of an atmospheric layer leading to saturation, a potentially stable layer will tend to form stratiform clouds, while a potentially unstable layer will produce cumuliform clouds and perhaps eventually convective precipitation (showers).

All the analyses of vertical stability considered so far have been summarized, for convenience, in Table IX-1.

* We notice that the conditions $\delta\theta_{aw}/\delta z \lesseqgtr 0$ refer here to the stratification of a layer, initially not saturated, which rises in the atmosphere, while conditions (44) referred to the environment, when a saturated parcel rises in it.

TABLE IX-1
Vertical stability

(A) Local stability conditions

Parcel method: $\gamma_v \lesseqgtr \gamma'_v = \begin{cases} \gamma_d, \text{ unsaturated}; & \text{or } \dfrac{\delta\theta}{\delta\phi} \lesseqgtr 0 \\ \gamma_w, \text{ saturated}; & \text{or } \dfrac{\delta\theta_{aw}}{\delta\phi} \lesseqgtr 0 \end{cases}$

Layer method: $(\gamma_v - \gamma') \gtreqless \dfrac{A'}{A}(\gamma - \gamma_v)$

where upper inequality signs correspond to instability, lower inequality signs correspond to stability, equality signs correspond to indifference.

$\gamma_v > \gamma_d$ *absolute instability*
$\gamma_d > \gamma_v > \gamma_w$ *conditional instability* → (B)
$\gamma_v < \gamma_w$ *absolute stability*

(B) Finite vertical displacements: *latent instability*

$A_+ > A_-$ real latent type
$A_+ < A_-$ pseudolatent type
$A_+ = 0$ stable type

(C) Layer vertical displacements: *potential or convective instability.*

Unsaturated: $\gamma'_v = \gamma_v + (\gamma_d - \gamma_v)\left(1 - \dfrac{p'A'}{pA}\right)$

$p'/p < 1$ ascent
$A'/A < 1$ lateral convergence
} → destabilization

$p'/p > 1$ descent
$A'/A > 1$ lateral divergence
} → stabilization

With saturation: $\dfrac{\delta\theta_{aw}}{\delta\phi} \lesseqgtr 0$ { potentially unstable (upper sign); potentially stable (lower sign)

9.11. Processes Producing Stability Changes for Dry Air

From Equation (40), (Chapter VIII, Equation (21)) and the gas law, it follows that, for dry air,

$$\frac{\delta \ln \theta}{\delta p} = -\frac{R_d}{p}(\gamma_d - \gamma). \tag{64}$$

This equation suggests that a useful stability parameter could be defined by the relation

$$\sigma = -\frac{\delta \ln \theta}{\delta p}, \tag{65}$$

with the associated stability criteria

$$\sigma \gtrless 0, \tag{66}$$

where, now, the sign $>$ corresponds to stability and $<$ to instability. At a fixed pressure, σ is a single-valued function of γ. Moreover, the finite-difference approximation to σ, $-\Delta \ln\theta/\Delta p$, is obtainable immediately from a tephigram curve.

At a fixed isobaric level, σ increases as the lapse rate decreases, i.e., as the stability increases; and σ decreases as the lapse rate increases, i.e., as the stability decreases. Thus, for increasing stability $(\partial\sigma/\partial t)_p > 0$, for decreasing stability, $(\partial\sigma/\partial t)_p < 0$. From Equation (65),

$$\left(\frac{\partial\sigma}{\partial t}\right)_p = \left[\frac{\partial}{\partial t}\left(-\frac{\partial \ln\theta}{\partial p}\right)\right]_p = -\frac{\partial}{\partial p}\left(\frac{\partial \ln\theta}{\partial t}\right)_p . \tag{67}$$

Our basic coordinate set is (x, y, p, t) and in terms of this set:

$$\frac{\mathrm{d} \ln\theta}{\mathrm{d}t} = \left(\frac{\partial \ln\theta}{\partial t}\right)_p + u\left(\frac{\partial \ln\theta}{\partial x}\right)_p + v\left(\frac{\partial \ln\theta}{\partial y}\right)_p + \frac{\mathrm{d}p}{\mathrm{d}t}\frac{\partial \ln\theta}{\partial p} \tag{68}$$

where u and v represent the x- and y-components of wind velocity (positive to east and north, respectively) and $\mathrm{d}p/\mathrm{d}t$ represents the vertical motion in isobaric coordinates, the total rate of change of pressure with time for a moving element of air. It can be related to the vertical velocity by an expansion of the total derivative in terms of the (x, y, z, t) coordinate set:

$$\frac{\mathrm{d}p}{\mathrm{d}t} = \frac{\partial p}{\partial t} + u\frac{\partial p}{\partial x} + v\frac{\partial p}{\partial y} + w\frac{\partial p}{\partial z} = \left(\frac{\partial p}{\partial t} + u\frac{\partial p}{\partial x} + v\frac{\partial p}{\partial y}\right) - g\varrho w \cong -g\varrho w . \tag{69}$$

The bracketed terms are relatively small and physically insignificant, as far as approach to saturation is concerned, i.e., they result in very small adiabatic temperature changes.

For dry adiabatic changes, $\mathrm{d} \ln\theta/\mathrm{d}t = 0$, and in general, from the first principle of thermodynamics,

$$\frac{\mathrm{d} \ln\theta}{\mathrm{d}t} = \frac{1}{c_p T}\frac{\delta Q}{\delta t}. \tag{70}$$

From Equations (65), (68) and (70),

$$\left(\frac{\partial \ln\theta}{\partial t}\right)_p = -\left[u\left(\frac{\partial \ln\theta}{\partial x}\right)_p + v\left(\frac{\partial \ln\theta}{\partial y}\right)_p\right] + \sigma\frac{\mathrm{d}p}{\mathrm{d}t} + \frac{1}{c_p T}\frac{\delta Q}{\delta t}. \tag{71}$$

From Equations (67) and (71),

$$\left(\frac{\partial\sigma}{\partial t}\right)_p = \frac{\partial}{\partial p}\left[u\left(\frac{\partial \ln\theta}{\partial x}\right)_p + v\left(\frac{\partial \ln\theta}{\partial y}\right)_p\right] - \frac{\partial}{\partial p}\left(\sigma\frac{\mathrm{d}p}{\mathrm{d}t}\right) - \frac{\partial}{\partial p}\left(\frac{1}{c_p T}\frac{\delta Q}{\delta t}\right). \tag{72}$$

The first term can be interpreted in two alternative ways. Since

$$\mathrm{d}\ln\theta = \mathrm{d}\ln T - \varkappa\,\mathrm{d}\ln p, \tag{73}$$

the first term can also be written as

$$\frac{\partial}{\partial p}\left[u\left(\frac{\partial \ln T}{\partial x}\right)_p + v\left(\frac{\partial \ln T}{\partial y}\right)_p\right],$$

and is thus related to the variation in the vertical of the horizontal (strictly speaking, isobaric) temperature advection. Thus this term could be called the differential isobaric advection term. It can be interpreted in a slightly different way by expansion, i.e.

$$\frac{\partial}{\partial p}\left[u\left(\frac{\partial \ln\theta}{\partial x}\right)_p + v\left(\frac{\partial \ln\theta}{\partial y}\right)_p\right] = \left[\frac{\partial u}{\partial p}\left(\frac{\partial \ln\theta}{\partial x}\right)_p + \frac{\partial v}{\partial p}\left(\frac{\partial \ln\theta}{\partial y}\right)_p\right] + \left[u\frac{\partial}{\partial p}\left(\frac{\partial \ln\theta}{\partial x}\right)_p + v\frac{\partial}{\partial p}\left(\frac{\partial \ln\theta}{\partial y}\right)_p\right]. \tag{74}$$

The second bracketed quantity can be rewritten, by interchanging the order of differentiation, as

$$u\left[\frac{\partial}{\partial x}\left(\frac{\partial \ln\theta}{\partial p}\right)\right]_p + v\left[\frac{\partial}{\partial y}\left(\frac{\partial \ln\theta}{\partial p}\right)\right]_p = -\left[u\left(\frac{\partial\sigma}{\partial x}\right)_p + v\left(\frac{\partial\sigma}{\partial y}\right)_p\right] \tag{75}$$

which is simply the isobaric advection of stability, a quasi-horizontal process. In the first bracketed quantity, $\ln\theta$ can again be replaced by $\ln T$ and the thermal wind equations of dynamic meteorology employed to introduce the isobaric shear of the geostrophic wind components $-\partial u_g/\partial p$ and $\partial v_g/\partial p$, i.e.,

$$\frac{\partial u}{\partial p}\left(\frac{\partial \ln T}{\partial x}\right)_p + \frac{\partial v}{\partial p}\left(\frac{\partial \ln T}{\partial y}\right)_p = -f\varrho\left(\frac{\partial u}{\partial p}\frac{\partial v_g}{\partial p} - \frac{\partial v}{\partial p}\frac{\partial u_g}{\partial p}\right), \tag{76}$$

where we denote by f the Coriolis parameter, $2\omega\sin\varphi$. This expression has a non-zero value only if there are cross-contour (i.e., acceleration) components of the horizontal wind field, and such effects are generally of minor importance. Thus, for quasi-geostrophic or quasi-gradient winds, the differential isobaric advection term implies merely the isobaric advection of stability.

For the benefit of those unfamiliar with the concept of the geostrophic wind, we will digress at this point to present a few formulae which illustrate and explain this concept, and from which the relation of the temperature field to the variation in the vertical of the geostrophic wind can be deduced. If we derive the equations of motion for a set of axes anchored to a rotating earth, neglect friction but take into account forces resulting from horizontal variations of pressure, we obtain the following wind-component equations:

$$u = u_g - \frac{1}{f}\frac{dv}{dt}; \qquad v = v_g + \frac{1}{f}\frac{du}{dt}. \tag{77}$$

Here u and v are the x- and y-components of the (actual) horizontal wind, and u_g and v_g the corresponding components of the geostrophic wind, a synthetic or theoretical wind, whose calculation is outlined below, and which serves as a very useful and simple approximation to the true wind. f denotes the Coriolis parameter, $2\omega \sin\varphi$ (ω = angular velocity of the earth, φ = latitude).

From set (77) we see that if there are no accelerations for either component (steady motion), the wind and the geostrophic wind, are identical. The latter can be obtained from the following equations, in which the hydrostatic equation has been used to convert horizontal gradients of pressure to isobaric gradients of geopotential:

$$u_g = -\frac{1}{f\varrho}\frac{\partial p}{\partial y} = -\frac{1}{f}\left(\frac{\partial \varphi}{\partial y}\right)_p; \qquad v_g = \frac{1}{f\varrho}\frac{\partial p}{\partial x} = \frac{1}{f}\left(\frac{\partial \varphi}{\partial x}\right)_p. \tag{78}$$

Since f at mid-latitudes is of the order of $10^{-4}\ s^{-1}$, it follows from Equation (77) that the difference between the actual wind and the geostrophic wind, in any direction, has a magnitude closely comparable to that of the change of the actual wind component in any orthogonal direction, following the motion, for a period of 3 h. Since a reasonable value of acceleration could be 50% of the velocity per day, departures of winds from geostrophic values would average less than 10%. For balanced motion in a circular path (total acceleration zero), the wind is known as the gradient wind.

The isobaric shear of the geostrophic wind (which is also a first approximation to the isobaric shear of the actual wind) can be found from set (78), by a differentiation with respect to pressure, making use of the hydrostatic equation and the ideal gas law:

$$\frac{\partial u_g}{\partial p} = -\frac{1}{f}\frac{\partial}{\partial p}\left(\frac{\partial \varphi}{\partial y}\right)_p = -\frac{1}{f}\left[\frac{\partial}{\partial y}\left(\frac{\partial \varphi}{\partial p}\right)\right]_p = \frac{1}{f}\left[\frac{\partial (1/\varrho)}{\partial y}\right]_p = \frac{R_d}{fp}\left(\frac{\partial T}{\partial y}\right)_p \tag{79}$$

$$\frac{\partial v_g}{\partial p} = \frac{1}{f}\frac{\partial}{\partial p}\left(\frac{\partial \varphi}{\partial x}\right)_p = \frac{1}{f}\left[\frac{\partial}{\partial x}\left(\frac{\partial \varphi}{\partial p}\right)\right]_p = -\frac{1}{f}\left[\frac{\partial (1/\varrho)}{\partial x}\right]_p = -\frac{R_d}{fp}\left(\frac{\partial T}{\partial x}\right)_p. \tag{80}$$

Equations (79) and (80) are known as the thermal wind equations, since they relate the thermal field to the change of geostrophic wind in the vertical. These are the equations employed to produce the result quoted in Equation (76).

The second term in the stability-parameter tendency Equation (72), the vertical motion term, can best be studied after further expansion into the form:

$$-\frac{\partial}{\partial p}\left(\sigma \frac{dp}{dt}\right) = -\frac{dp}{dt}\frac{\partial \sigma}{\partial p} - \sigma \frac{\partial}{\partial p}\left(\frac{dp}{dt}\right). \tag{81}$$

The first of these two terms represents simply the vertical advection of stability, while the second represents the effects of the vertical shrinking or stretching of an air column, i.e., the change in $\sigma = -\Delta \ln\theta/\Delta p$ when $\Delta \ln\theta$ remains constant, for dry adiabatic changes, but Δp changes (see Section 10.1.).

The third term in the stability tendency equation expresses the effect of vertical variations in non-adiabatic heating. In the free atmosphere, away from clouds or the Earth's surface, this effect will be small, except possibly near the tropopause or similar discontinuity in lapse rate and hence in the degree of turbulent mixing. Near the ground, the radiative $\delta Q/\delta t$ decreases in magnitude with height, as was pointed out in an earlier section, so that a pronounced diurnal cycle of the lapse rate exists in the lower layers of the atmosphere.

Before considering illustrations on schematic tephigrams of the vertical motion processes, it will be instructive to examine the degree of conservatism of stability, as measured by the parameter σ, and to consider typical vertical-motion distributions in the vertical. We shall first obtain a relation for the change of stability following the motion, $\mathrm{d}\sigma/\mathrm{d}t$, for quasi-gradient flow and quasi-adiabatic conditions. Collecting component terms for $(\partial\sigma/\partial t)_p$ from the expansions in Equations (72), (74), (75), (76), and (81), it follows that

$$\frac{\mathrm{d}\sigma}{\mathrm{d}t}=\left(\frac{\partial\sigma}{\partial t}\right)_p+u\left(\frac{\partial\sigma}{\partial x}\right)_p+v\left(\frac{\partial\sigma}{\partial y}\right)_p+\frac{\mathrm{d}p}{\mathrm{d}t}\frac{\partial\sigma}{\partial p}=-\sigma\frac{\partial}{\partial p}\left(\frac{\mathrm{d}p}{\mathrm{d}t}\right). \tag{82}$$

From the hydrodynamical equation of continuity (a mathematical expression of the law of conservation of mass), the shrinking or stretching of a moving air column can be related to the accumulation or depletion of mass associated with velocity gradients in isobaric surfaces such that

$$-\frac{\partial}{\partial p}\left(\frac{\mathrm{d}p}{\mathrm{d}t}\right)=\left(\frac{\partial u}{\partial x}\right)_p+\left(\frac{\partial v}{\partial y}\right)_p. \tag{83}$$

Equation (83), the equation of continuity in isobaric coordinates, expresses the fact that there can be no mass change between fixed isobaric surfaces. The quantity on the right is known as the isobaric divergence, when positive, and the isobaric convergence, when negative, these terms implying depletion and accumulation of mass, respectively. The expression is also referred to, quite generally, as the isobaric velocity divergence, and expresses the rate of change of mass by quasi-horizontal motions (outflow minus inflow). The term on the left of Equation (83) expresses the effect of motions through isobaric surfaces in changing the mass of a layer.

It follows from Equations (82) and (83) that

$$\frac{\mathrm{d}\ln\sigma}{\mathrm{d}t}=\left(\frac{\partial u}{\partial x}\right)_p+\left(\frac{\partial v}{\partial y}\right)_p. \tag{84}$$

Thus isobaric divergence corresponds to an increase in magnitude of σ, and isobaric convergence to a decrease in magnitude of σ. It is clear, however, that no mechanism exists for changing stability to instability in a moving element of air, and that instability can only be produced locally if it existed previously upstream. Since instability will rapidly be destroyed by convective turbulent mixing (leading to $\gamma=\gamma_d$), it follows that super-adiabatic lapse rates must have an extremely ephemeral existence. However, it

should be emphasized that significant consequences of the release of instability are generally associated only with the condensation process (convective clouds, showers and thunderstorms). For saturated air there are different criteria for instability – the release of latent heat energy must be taken into account – and in general a combined dynamic–thermodynamic analysis is required. This topic will be considered further in the next section.

From Equation (69), $\mathrm{d}p/\mathrm{d}t \cong -g\varrho w$, it follows that, over level ground, $\mathrm{d}p/\mathrm{d}t$ is essentially zero at the surface. Integrating the equation of continuity from the surface (p_0) to an arbitrary level:

$$\frac{\mathrm{d}p}{\mathrm{d}t} = \int_{p}^{p_0} \left(\frac{\partial u}{\partial x} + \frac{\partial v}{\partial y}\right)_p \mathrm{d}p\,. \tag{85}$$

Thus, in a stratum of divergence at and above the surface, $\mathrm{d}p/\mathrm{d}t$ will be positive, corresponding to subsidence ($w<0$); in a stratum of convergence at and above the surface, $\mathrm{d}p/\mathrm{d}t$ will be negative, corresponding to ascent ($w>0$). Vertical motion studies have revealed that on the average a rather simple pattern of vertical motions may be expected in the troposphere. In general, tropospheric vertical motions tend to have the same sign, with a maximum absolute value in the mid-troposphere, in the vicinity of the 600 mb level, on the average. At this level of maximum (or minimum) $\mathrm{d}p/\mathrm{d}t$, the isobaric divergence must be zero, and this level is generally referred to as the level of nondivergence (L.N.D.). In any individual case, this level may depart appreciably from 600 mb, and does not in any event coincide with a specific isobaric surface, over any great area, at least. Moreover, especially in complex atmospheric situations, there may well be more than one level of non-divergence in the troposphere. However, the broad behavior of the troposphere is usually consistent with the existence of a single level of non-divergence in the mid-troposphere, either with divergence below and convergence above (subsidence) or with convergence below and divergence above (ascent).

We have already seen that divergence in a stable atmosphere will tend to increase the stability (decrease the lapse rate) and that convergence in a stable atmosphere will tend to decrease the stability (increase the lapse rate), both such rates being proportional to the initial value of the stability. Thus, for small stability ($(\gamma_d - \gamma)$ small) the effects of a given divergence or convergence on the stability will be small, while for large stability ($(\gamma_d - \gamma)$ large) the effects will be much greater (cf. Section 10.1). It is of interest to apply this concept, together with the normal divergence-convergence pattern of the atmosphere, to a consideration of the relative sharpness of frontal discontinuities as seen on atmospheric soundings on aerological diagrams. The significant discontinuity, charted as the front on quasi-horizontal analyses, is the upper boundary of the transition zone of intense isobaric thermal gradients, separating the stratum of great stability (σ large) characterizing this zone from the warm air mass above of normal stability (σ relatively small). The discontinuity in stability at this level may be taken as a measure of the sharpness of the front on the plotted sounding.

Since isobaric divergence increases the stability in the transition zone more rapidly than in the warm air, it will sharpen the frontal discontinuity. Since isobaric convergence decreases the stability in the transition zone more rapidly than in the warm air, it will weaken the frontal discontinuity. It is reasonable to expect that these effects would be visible, at least on the average, and synoptic experience does indeed verify the following conclusions.

Tropospheric ascent:

$$\left\{\begin{array}{l}\text{cold front, slow moving with persistent weather}\\ \text{warm front, normal activity re weather}\end{array}\right\}\ \left\{\begin{array}{l}\text{convergence below L.N.D.}\\ \text{divergence above L.N.D.}\end{array}\right\}$$

$$\left\{\begin{array}{l}\text{lower troposphere – frontal discontinuity relatively weak}\\ \text{upper troposphere – frontal discontinuity relatively sharp}\end{array}\right\}.$$

Tropospheric subsidence:

$$\left\{\begin{array}{l}\text{cold front, rapidly moving with rapid clearing}\\ \text{warm front, virtually no weather}\end{array}\right\}\ \left\{\begin{array}{l}\text{divergence below L.N.D.}\\ \text{convergence above L.N.D.}\end{array}\right\}$$

$$\left\{\begin{array}{l}\text{lower troposphere – frontal discontinuity relatively sharp}\\ \text{upper troposphere – frontal discontinuity relatively weak}\end{array}\right\}.$$

Let us consider now a typical situation with ascent throughout the troposphere, with isobaric convergence in the lower troposphere and divergence in the upper troposphere, as it might appear on an aerological diagram, neglecting horizontal advective processes (Figure IX-16).

In the upper troposphere $\partial/\partial p(\mathrm{d}p/\mathrm{d}t)<0$, and $\sigma>0$, so $\partial\sigma/\partial t>0$ (increasing stability). In the lower troposphere $\partial/\partial p(\mathrm{d}p/\mathrm{d}t)>0$, and $\sigma>0$, so $\partial\sigma/\partial t<0$ (decreasing stability).

Two weak discontinuities in lapse rate (and stability) are produced by this pattern of ascending motion and adiabatic cooling, and the new sounding may appear to contain a frontal discontinuity (at high levels), comparable to the passage of a weak

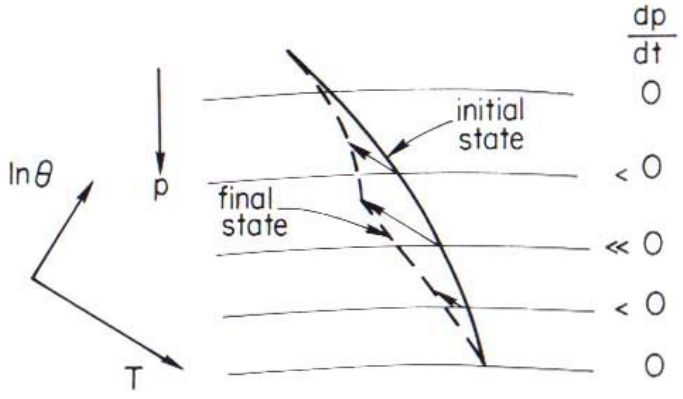

Fig. IX-16. Stability changes with isobaric convergence in the lower troposphere and divergence in the upper troposphere.

cold front. This phenomenon is often observed in advance of cold fronts especially when the warm air mass is relatively dry so that dry adiabatic cooling can take place; for this reason the phenomenon is known as 'pre-frontal cooling'. It can be distinguished from true frontal cooling, with a new and colder air mass below the front, by two distinguishing characteristics. In the first place, the cooling is relatively small in the lower portion of the sounding (effectively zero at the ground in the absence of advection), and, in the second place, the humidity increases at any level as the temperature drops. Thus it is always possible to obtain the new sounding by the ascent of typical warm air.

Let us consider now a typical subsidence situation, illustrated on a tephigram (Figure IX-17).

In the upper troposphere, $\partial/\partial p(\mathrm{d}p/\mathrm{d}t)>0$ and $\sigma>0$, so that $\partial\sigma/\partial t<0$ (decreasing stability). In the lower troposphere, $\partial/\partial p(\mathrm{d}p/\mathrm{d}t)<0$ and $\sigma>0$, so that $\partial\sigma/\partial t>0$ (increasing stability). Once again a discontinuity in lapse rate has been produced by the pattern of descending motion and adiabatic warming, somewhat comparable to a warm front situation. Since the inversion has been produced by subsidence, it is known as a subsidence inversion. It can be distinguished from a true warm frontal

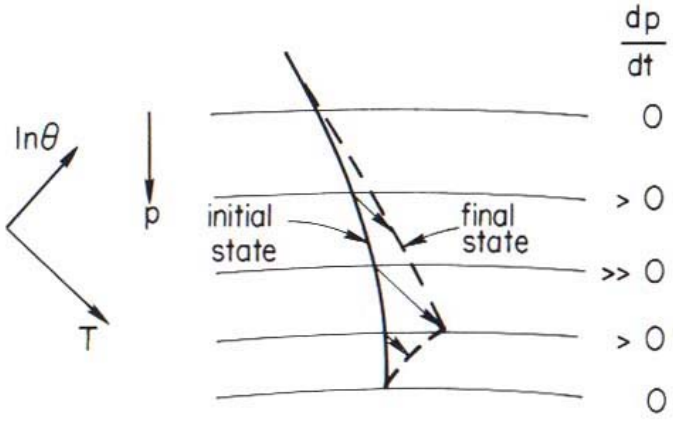

Fig. IX-17. Stability changes associated with subsidence.

passage by the relatively slight warming in the upper troposphere, the steep lapse rate (small stability) above the inversion, and by the low humidities that will appear near the top of the inversion layer. One can, of course, obtain representative temperatures and dewpoints by the ascent of the relatively dry air (in nature, or by carrying it out on the diagram).

9.12. Stability Parameters of Saturated and Unsaturated Air, and Their Time Changes

If we had maintained the effects of water vapor in the derivations of the last section (i.e., starting from Equation (40)), we might have defined a virtual stability parameter for unsaturated air as

$$\sigma_v = -\frac{\delta \ln \theta_v}{\delta p} = \frac{R_d}{p}(\gamma_d - \gamma_v). \tag{86}$$

All the relations in Section 11 would still be valid, with the subscript v as above, with quite acceptable accuracy. For most practical purposes, such refinements are unnecessary since the virtual temperature increments for a vertically-moving parcel and for its environment at any time would differ by only a few tenths of a degree Celsius, in general.

When dealing with saturated air, numerous complications arise, which generally introduce uncertainties in the temperature (or virtual temperature) of a parcel which exceed the virtual temperature increment differential between parcel and environment. In the first place, one will not know whether ascent is of the saturated adiabatic or pseudo-adiabatic category. Initial saturation is almost invariably followed by cloud development without precipitation (a saturated adiabatic process), and only later, when additional physical criteria are satisfied, may precipitation occur (a pseudo-adiabatic process). For the truly reversible process, the (p, T) variation depends on the initial condensation level and the virtual temperature will now depend on the concentration of condensed water as well as of water vapor. Since the volume occupied by the condensed phase is negligible, the virtual temperature of the cloud air (incorporating the effect of the condensed phase as a component of the air) is given by an extension of the treatment in Chapter IV, Section 11 as

$$T_v = \frac{T(1 + r_w/\varepsilon)}{(1 + r_w)} \frac{1 + r_w}{1 + r_w + r_l} = \frac{T(1 + r_w/\varepsilon)}{(1 + r_t)}. \tag{87}$$

These various effects are by no means compensatory. Moreover, once the temperature of an ascending parcel falls below 0 °C, additional uncertainties are introduced with respect to the level (if any) at which the transition from water-saturation to ice-saturation takes place. If we imagine a large ascending mass of air, of cloud dimensions, the micro-processes that take place inside the cloud will greatly affect stability considerations. We must conclude, then, that the stability or instability of saturated air can only be handled in its grosser aspects by a pure thermodynamic analysis.

If we have a parcel of saturated air, it will be stable relative to its environment (saturated or unsaturated) provided that $\gamma < \gamma_s$, where γ_s is some sort of saturated adiabatic lapse rate (true or pseudo, relative to water or ice). If $\gamma > \gamma_s$, the parcel will exhibit instability (analogous to dry-air instability when $\gamma > \gamma_d$). Since $\gamma_s < \gamma_d$, a layer of unsaturated air may itself be stable, but will still accelerate the vertical motions of a saturated parcel, if $\gamma_s < \gamma < \gamma_d$. This we have defined (in Section 5) as conditional instability, since it depends on the state of a moving parcel. If it is possible for a moving air parcel, on adiabatic ascent to and beyond saturation, to achieve the temperature of the environment at some level, the instability is then known as latent instability (see Section 6). If the conditional instability criterion ($\gamma_d > \gamma > \gamma_s$) is to be expressed in terms of the vertical gradient of some specific property of the air, the appropriate property must relate to the saturation or pseudo-adiabat through (p, T).